

Heidi Soosalu · Páll Einarsson · Steinunn Jakobsdóttir

## Volcanic tremor related to the 1991 eruption of the Hekla volcano, Iceland

Received: 14 February 2002 / Accepted: 12 February 2003 / Published online: 4 April 2003  
© Springer-Verlag 2003

**Abstract** Volcanic tremor at the Hekla volcano is directly related to eruptive activity. It starts simultaneously with the eruptions and dies down at the end of them. No tremor at Hekla has been observed during non-eruptive times. The 1991 Hekla eruption began on 17 January, after a short warning time. Local seismograph stations recorded small premonitory earthquakes from 16:30 GMT on. At 17:02 GMT, low-frequency volcanic tremor became visible on the seismograph records, marking the onset of the eruption. The initial plinian phase of the eruption was short-lived. During the first day several fissures were active but, by the second day, the activity was already limited to a segment of one principal fissure. The eruption lasted almost 53 days. At the end of it, during the early hours of 11 March, volcanic tremor disappeared under the detection threshold and was followed by a swarm of small earthquakes. At the start of the eruption, the tremor amplitude rose rapidly and reached a maximum in only 10 min. The tremor was most vigorous during the first hour and started to decline sharply during the next hour, and later on more gently. During the eruption as a whole, the tremor had a continuous declining trend, with occasional increases

lasting up to about 2 days. Spectral analysis of the tremor during the first 7 h of the eruption shows that it settled quickly, within a couple of minutes, to its characteristic frequency band, 0.5–1.5 Hz. The spectrum had typically one dominant peak at 0.7–0.9 Hz, and a few subdominant peaks. Hekla tremor likely has a shallow source. Particle motion plots suggest that it contains a significant component of surface waves. The tremor started first when the connection of the magma conduit with the atmosphere was reached, suggesting that degassing may contribute to its generation.

**Keywords** Hekla eruption 1991 · Volcanic tremor · Earthquakes · Eruption monitoring

### Introduction

Hekla is one of the most active volcanoes of Iceland. It has erupted at least 18 times since Iceland was inhabited approximately 1,100 years ago (Guðmundsson et al. 1992). Hekla is located in south Iceland at the junction of the south Iceland seismic zone and eastern volcanic zone (Fig. 1). It is an ENE-WSW-trending ridge built up to the height of 1,500 m above sea level by repeated eruptions on a narrow fissure zone. The products are mainly basaltic and andesitic lavas and tephra (Þórarinnsson 1967).

The eruption history of Hekla since the settlement time has in several ways been quite regular—in regard to durations of events, repose periods separating them, and amount and composition of volcanic products. Large eruptions have typically occurred twice per century, the average repose period being 55 years (Þórarinnsson 1967; Guðmundsson et al. 1992). A new pattern has emerged in the last half-century, with smaller and more frequent eruptions in 1970, 1980–1981, 1991, and 2000. Only very short seismic precursors have been noticed before these eruptions. The seismicity related to them has started very gradually and has reached the detection threshold 25–80 min before their onset (Einarsson and Björnsson 1976;

Editorial responsibility: J.F. Lénat

H. Soosalu (✉)  
Institute of Seismology,  
University of Helsinki,  
Teollisuuskatu 23, P.O. Box 26, 00014 Helsinki, Finland  
e-mail: heidi@hi.is  
Fax: +354-562-9767

P. Einarsson  
Science Institute,  
University of Iceland,  
Hofsvallagata 53, 107 Reykjavík, Iceland

S. Jakobsdóttir  
Icelandic Meteorological Office,  
Bústaðavegur 9, 150 Reykjavík, Iceland

*Present address:*

H. Soosalu, Nordic Volcanological Institute,  
Grensásvegur 50, 108 Reykjavík, Iceland

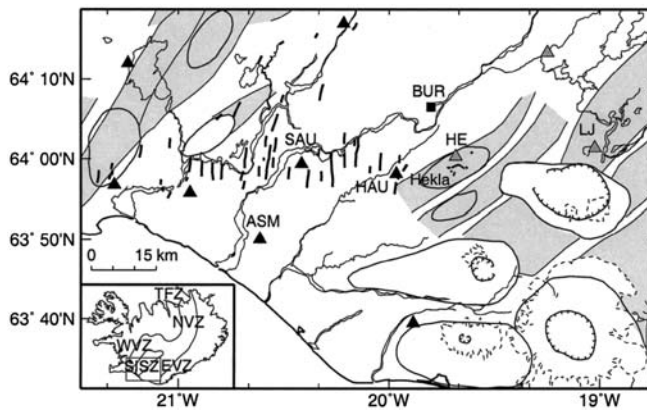


**Fig. 1** Index map of the Hekla region. *Closed triangles* are the digital seismograph stations of the South Iceland Lowland (SIL) network, and *shaded triangles* the analog stations. The stations which are used in this study are named in the map. *The closed square* is the strain station BUR of Linde et al. (1993). The central volcanoes are outlined, and their fissure swarms *shaded* (Einarsson and Saemundsson 1987) and the calderas *hatched* (Jóhannesson et al. 1990). *Thick solid lines* are the faults of the South Iceland seismic zone. *Thick solid lines* inside the Hekla central volcano show the 1991 eruptive sites. *Dashed lines* mark the glaciers, *thin lines* lakes and rivers. The small *index map* shows the locations of the western (WVZ), eastern (EVZ) and northern (NVZ) volcanic zones, the South Iceland seismic zone (SISZ), and the Tjörnes fracture zone (TFZ). All the figures are drawn using the Generic Mapping Tools program (Wessel and Smith 1998)

Grönvold et al. 1983; Guðmundsson et al. 1992; Einarsson 2000; Stefánsson et al. 2000).

In spite of the general lack of earthquakes, Hekla eruptions appear to be accompanied by persistent volcanic tremor. The tremor is easily observed and provides an important parameter for monitoring purposes. The 1991 eruption is the first one for which there exist digital seismic data, suitable for a meaningful quantitative study of tremor. In this paper we attempt to describe the 1991 tremor, its characteristics, time history, and relation to the eruption, using three digital and two analog seismic stations. Sound knowledge of this is a prerequisite for a successful alert system based on seismic observations.

### Previous studies on earlier Hekla eruptions

The Hekla eruption in 1970 started on 5 May at about 21:23 GMT, when fissures opened on the SSW and W flanks of Hekla (Þórarinnsson and Sigvaldason 1972). At that time there were only three permanent seismic stations in Iceland, at 80-, 110- and 200-km distances from Hekla. The stations started to record continuous tremor at 20:58, about 25 min before the onset of the eruption. The tremor amplitude increased steadily until 21:18 when there was a sudden burst of tremors. Subsequently, numerous bursts occurred superimposed on the continuous tremor (Einarsson and Björnsson 1976). In retrospect, it seems likely that the tremor was made by superposition of numerous small earthquakes.

The Hekla eruption in 1980 began on 17 August. Earthquake activity related to it started to show up at 13:04. Continuous movement resembling a series of small earthquakes was recorded at about 13:10. Definite volcanic tremor was recorded from 13:27 on, about the same time as the beginning of the eruption. It reached maximum amplitude during the next hour but started to decrease again at about 16:00. The amplitude followed the tephra production rate. In general, during the eruption the amplitude of the tremor appeared to follow the vigour of the volcanic activity (Grönvold et al. 1983; Brandsdóttir and Einarsson 1992).

The 1980 eruption lasted until 20 August but activity at Hekla resumed in April 1981. Volcanic tremor similar to the August tremor was noticeable on a seismometer shortly after 22:00 on 8 April. The tremor amplitude increased rapidly between 02:00 and 05:00 in the morning of 9 April when the first tephra fall was noted. However, the weather conditions prevented direct observations of the eruption site. The tremor started to decrease slowly in the morning of 10 April, and finally disappeared below the detection level on 16 April with the last signs of the eruption (Grönvold et al. 1983).

### The seismograph stations observing the volcanic tremor of the 1991 Hekla eruption

The Nordic seismological South Iceland Lowland (SIL) project was started in 1988 for purposes of earthquake prediction research in the south Iceland seismic zone (Stefánsson et al. 1993). The SIL network of eight, digital, three-component seismograph stations located in the South Iceland Lowland (Fig. 1), west of Hekla, began to collect data in the year 1990. The instrumentation consisted of Lennartz LE-3D/1 s seismometers and Nanometrics RD3 digitizers. The Hekla eruption was the first significant geophysical event occurring during the operation of this network.

The eruption started on 17 January 1991, after a short warning time. The SIL stations recorded premonitory earthquakes (Stefánsson et al. 1993; Soosalu and Einarsson 2002), and subsequently volcanic tremor associated with the beginning of the eruption. The initial plinian phase of the eruption was short-lived. Several fissures were active during the first day. By the second day, the activity was already limited to a segment of one principal fissure where the main crater subsequently formed. This eruption lasted almost 53 days, until 11 March (Guðmundsson et al. 1992).

During the first hours of the eruption, the station SAU at 35-km distance (see Fig. 1) provides the main source for tremor data. Continuous datasets recorded by SAU, and by the station ASM 50 km from Hekla, until about midnight of 17 January, are available. Unfortunately the closest station at the onset of the eruption, SAU, is already quite a distance from Hekla. However, we can see many characteristic features of the tremor in its records. HAU, the digital station nearest to Hekla, 15 km away,

was down when the eruption broke out, as a new software version was being installed there. Only a 47-s data sample was saved at HAU at 20:27 GMT on 17 January. During the eruption as a whole, the HAU data are the main material for tremor analysis.

Analog vertical component seismograph stations also operated in the region during the eruption (Fig. 1), and they provide material for more qualitative analysis of the volcanic tremor. The analog station LJ has continuous tremor records for the first days of the eruption, until its amplitude faded under the detection threshold. The station HE on the flank of Hekla itself was out of order during the first part of the eruption. From 24 February on, it gives account of the behaviour of the tremor during the last days of the eruption.

---

### Time history of the eruption in the light of tremor observations

Hekla is known to be typically aseismic during volcanically quiet times (Einarsson 1991). In accordance with this, no earthquakes were observed at Hekla before 17 January, and thus there are no signs of precursory seismicity. Numerous small earthquakes were related to the onset of the eruption (Soosalu and Einarsson 2002). Sixty earthquakes were observed by the SIL system before the onset of the eruption (16:30–17:01 GMT), and 320 events between 17:02 and midnight (see below). The low-frequency volcanic tremor appears on the seismograms at 17:02 GMT (see below), showing that the eruption had started.

According to Guðmundsson et al. (1992), the eruption started at about 17:00. They mention that a rising eruption column was first seen from a nearby farm at 17:05. Linde et al. (1993) state that the surface breakout of the eruption is not determined precisely by visual or other direct observation. Their strain measurements show clear strain changes due to magma movement from 16:36 on. They inferred the surface breakout to be at 17:01 (Linde et al. 1993; Stefánsson et al. 1993), consistent with our conclusion.

The eruption was by far most vigorous during the first day, and several fissures were active. According to eyewitness accounts, the eruption attained its peak about one hour after the start, and was subsequently on decline. Effusion of lava began simultaneously with, or shortly after, the explosive activity. By the second day of eruption, the activity was already mainly restricted to a single fissure on the lower south flank, trending southeast from the top of Hekla. Slight activity in another fissure on the south side of the volcano lasted until 20 January (Guðmundsson et al. 1992).

The amplitude of the volcanic tremor rose rapidly and stayed highest during the first hour. The maximum reduced displacement (e.g. McNutt 1994a) calculated from the records of the station SAU was about 8 cm<sup>2</sup>. The effusion rate of lava (see below), a basaltic andesite, may have reached a peak of 2,000 m<sup>3</sup>/s during the first day.

The average effusion rate during the first two days was 800 m<sup>3</sup>/s. Later on the rate declined rapidly to 10–20 m<sup>3</sup>/s, then more slowly to 1 m<sup>3</sup>/s, and remained at 1–12 m<sup>3</sup>/s until the end. The volcanic tremor diminished rapidly in the evening of 10 March, and disappeared into the background noise around 05:00 on 11 March. The eruption most likely came to an end around noon on 11 March (Guðmundsson et al. 1992).

In the case of Hekla, the volcanic tremor appears to more or less reflect the eruptive activity. It starts simultaneously with the eruptions and dies away towards the end of the eruptions, together with the volcanic activity (Einarsson and Björnsson 1976; Grönvold et al. 1983; Guðmundsson et al. 1992). No tremor has been observed from Hekla during non-eruptive times. This behaviour is not self-evident for every volcano. Some volcanoes show periods of volcanic tremor without observable eruptive activity (Schick 1988). At Etna, for example (e.g. Montalto et al. 1995), tremors are recorded a long time before visible volcanic activity and probably can be used as a tool for eruption prediction.

After the first hours of the Hekla eruption, the swarm of numerous, small earthquakes died out and the volcanic tremor was the main seismic expression of the eruption. During later phases of the eruption, earthquakes at Hekla were few (further details of the earthquake seismicity are given by Soosalu and Einarsson 2002).

---

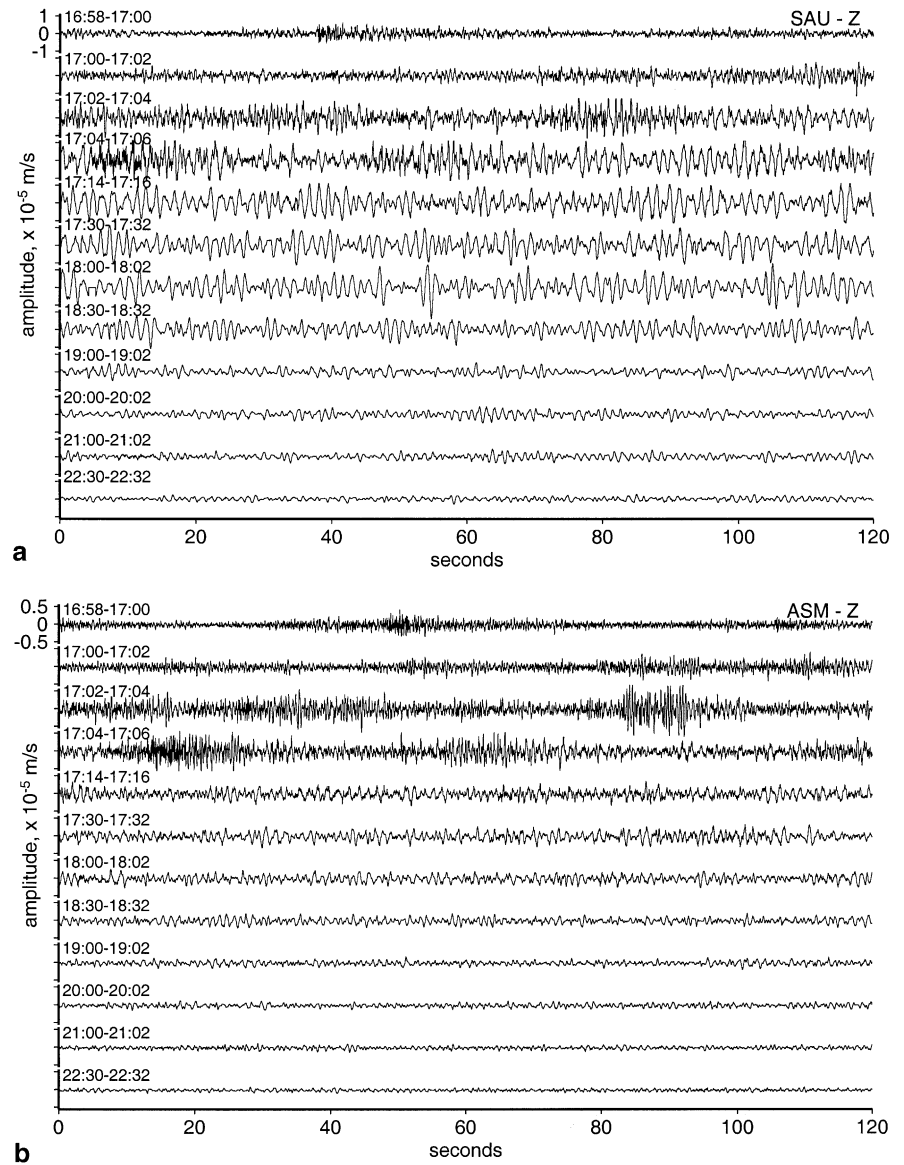
### Tremor observations for the first hours of the eruption

Representative samples of seismograms of SAU and ASM during the first hours are presented in Fig. 2a, b. During the first minutes of the assumed start of the eruption, higher frequencies (i.e. earthquakes) are distinct on the seismograms. Low-frequency volcanic tremor starts to be visible first between earthquakes and then as a dominating factor from ~17:05 on. The amplitude of the tremor oscillates. Episodes of high-amplitude tremor, lasting from some seconds to about 10 s, are separated by moments of lower amplitude. This pattern is preserved until midnight.

The tremor amplitude rises high rapidly after the onset of the eruption. The maximum is reached only about 10 min after the start. From then on, the amplitude remains high for about 1 h. Shortly before 18:00 it begins to decline. From 18:00 on, the decline is quite rapid and this tendency continues until 18:40–18:50. Subsequently, the tremor declines much more slowly.

On the ASM seismograms the tremor is not as outstanding as it is on SAU, although its general appearance is similar. During the first minutes the numerous earthquakes related to the onset of the eruption dominate the appearance of the ASM seismograms. Later on the low-frequency tremor is clearly visible and remains in the seismograms until midnight. However, its amplitude diminishes quickly; there is a clear change already after the first hour of the eruption.

**Fig. 2** **a** Representative 2-min-long samples of SAU vertical component records at the time of the onset of the Hekla eruption, 17 January 1991. The amplitude scale is the same for every sample. **b** Representative samples of ASM vertical component records, times same as at SAU. The amplitude scale is the same for every ASM sample, and twice the scale of the SAU samples. No filtering is done. The seismometer instrumentation is the same at both SAU and ASM



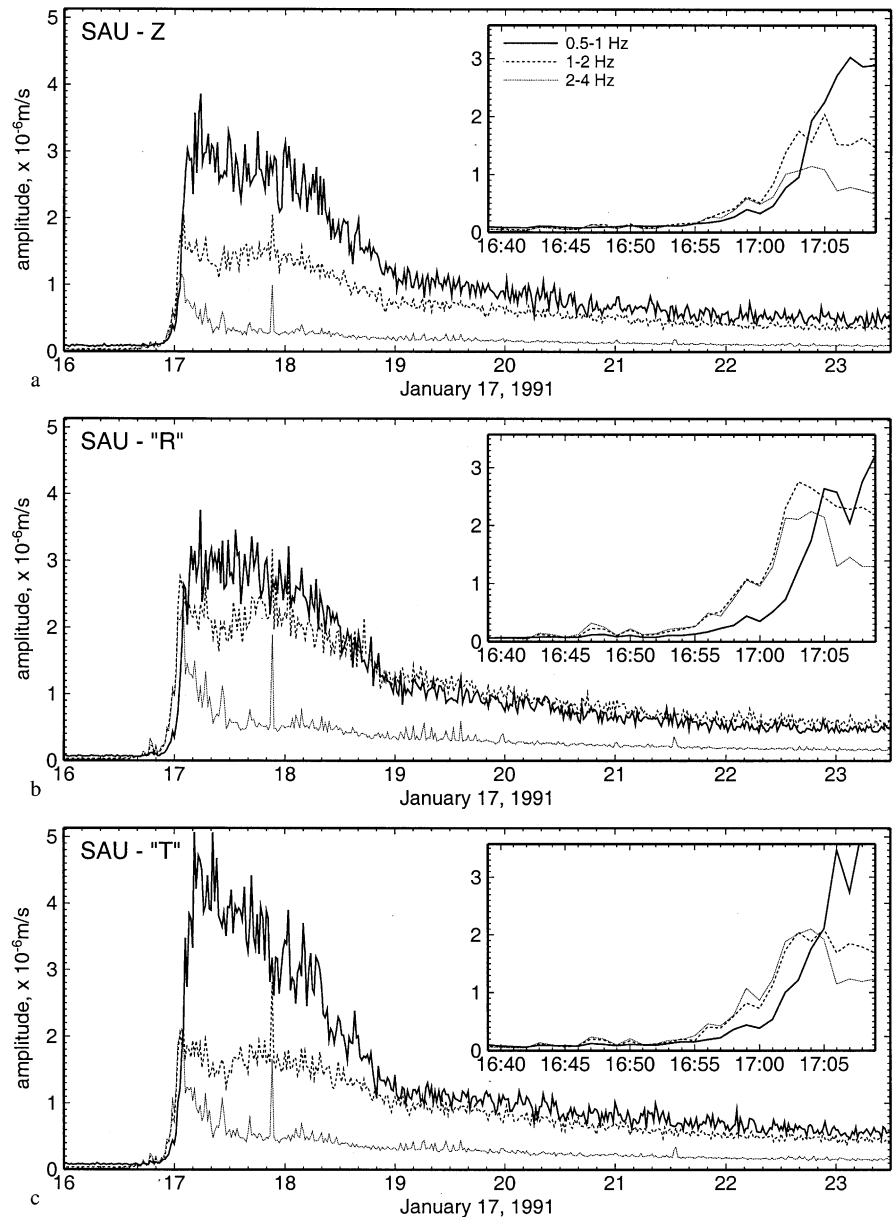
Figures 3a–c and 4a–c show the temporal development of three frequency bands of SAU and ASM data; both the vertical and the two horizontal components are shown. As the station SAU is located west of Hekla, its east component was readily taken as the radial, and its north component as the transverse component. The horizontal components of the station ASM were rotated 20° counter-clockwise to approximately obtain the radial and the transverse components. The frequency bands 0.5–1.0, 1.0–2.0, and 2.0–4.0 Hz were considered relevant for separating the fingerprints of the tremor (primarily the 0.5–1.0 Hz band) and the numerous earthquakes (the higher frequencies). The insets show the behaviour in the very beginning. At 17:02–17:03 GMT there is a sudden increase in the 0.5–1.0 Hz tremor build-up, simultaneously with a decrease in the higher frequencies which indicates decrease in earthquake activity. This suggests

that the fissure has stopped propagating and the magma has a free path to the surface.

The tremor waves (low frequencies) attenuate more with distance than the earthquake waves (higher frequencies). This is well visible both in the seismograms (Fig. 2a, b) and in the attenuation of the different frequency bands in Fig. 3a–c of SAU and Fig. 4a–c of the more distant ASM.

The behaviour of the tremor during the first hours of the eruption is quantitatively presented in a graph expressing its intensity at SAU and ASM (Fig. 5a). The vertical component data are used and band-pass filtered between 0.5 and 5.0 Hz to eliminate the effect of the microseism in the lower end and of the earthquakes in the higher end. The intensity is calculated as averaged energy over 60-s intervals. Its ln logarithm in function of time is plotted on the graph. The general intensity pattern at both stations is similar but overall smaller values of ASM are

**Fig. 3a–c** Tremor amplitude time series with different frequency bands, 0.5–1.0 Hz (*solid line*), 1.0–2.0 Hz (*dashed line*), and 2.0–4.0 Hz (*dotted line*) for the station SAU: **a** the vertical, **b** the “radial” (E–W), and **c** the “transverse” (N–S) component. The values are one-minute amplitude averages. The *insets* show the behaviour of the frequency bands around the very onset of the eruption

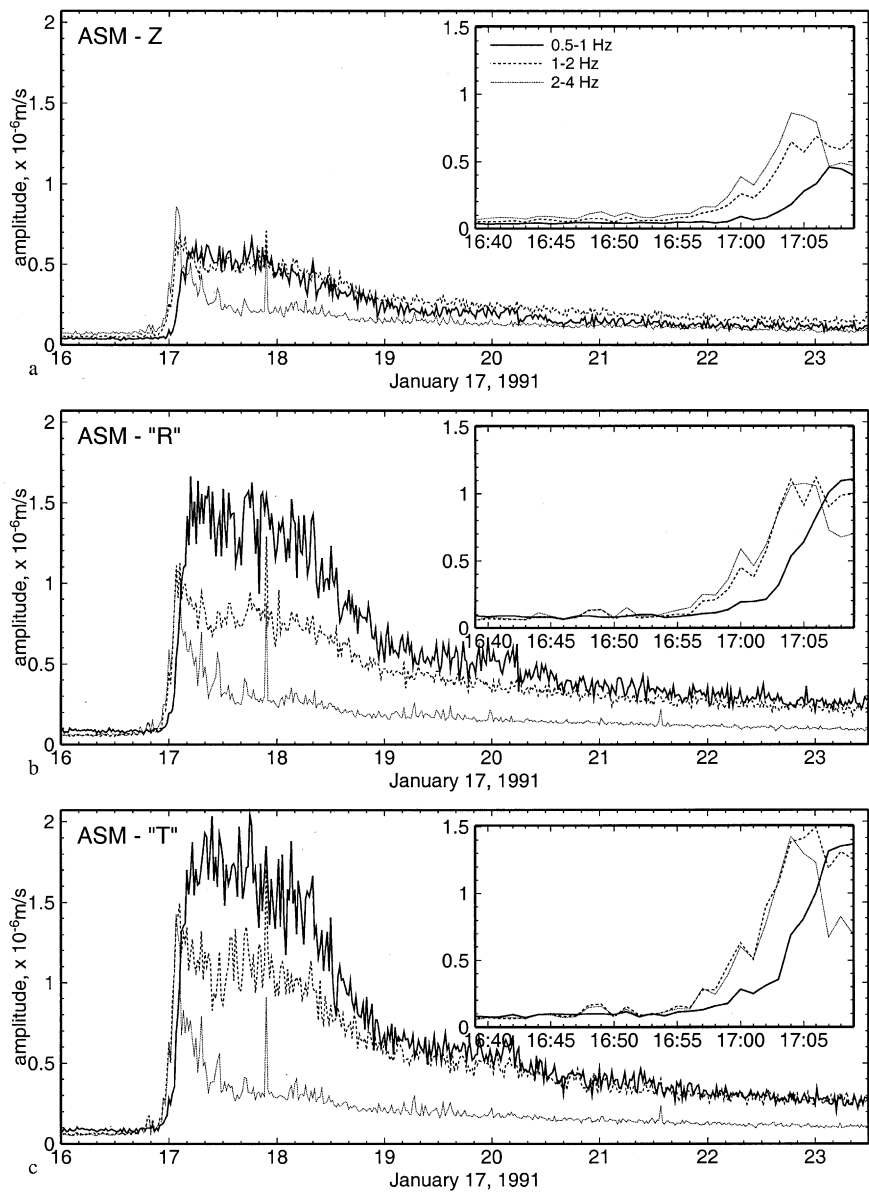


due to greater distance. The continuous fluctuation of the intensity throughout the time period is also common for both. The earthquakes observed until midnight are in the same plot for comparison.

At the onset of the eruption the intensity at SAU and ASM jumps quickly, in matter of minutes, to high levels. The intensity remains high during the first hour. At 18:10–18:20 it turns to a sharp decline which continues to about 19:00. At that time there is a clear bend in both of the diagrams, after which the intensity declines more gently towards midnight. For comparison to the intensity graphs, a more qualitative amplitude plot measured from paper seismograms of the analog station LJ is drawn in Fig. 5b. Tremor amplitudes and their decline at LJ follow a similar pattern as the intensities at SAU and ASM.

Linde et al. (1993) analysed data from a strain station network in the vicinity of Hekla during the eruption. They observed at the nearest station, BUR, 15 km from Hekla (see Fig. 1), remarkable contraction from the time before 16:40 on. This continued until 18:40 when a minimum was reached and the strain turned to expansion. The more distant stations, 37–45 km from Hekla, showed solely expansion during the first two days of the eruption. They interpreted this as two stages, of which the first one is characterized by deflation of a deep reservoir (seen by the distant stations) together with dyke formation (seen only by the nearest station). The second stage, starting at 18:40, consists only of deflation of the deep source which is observed by all the stations. The turning point of the strain data at the nearest station is not reflected in an obvious manner in the seismic intensity graphs (Fig. 5a),

**Fig. 4a–c** Tremor amplitude time series with different frequency bands, 0.5–1.0 Hz (*solid line*), 1.0–2.0 Hz (*dashed line*), and 2.0–4.0 Hz (*dotted line*) for the station ASM: **a** the vertical, **b** the “radial”, and **c** the “transverse” component (horizontal rotated 20° counter-clockwise from original). The *insets* show blowups of the onset of the eruption



as the quick decline of intensity slows down not until some 20 min later. However, the strain reversal coincides with a local minimum of earthquakes.

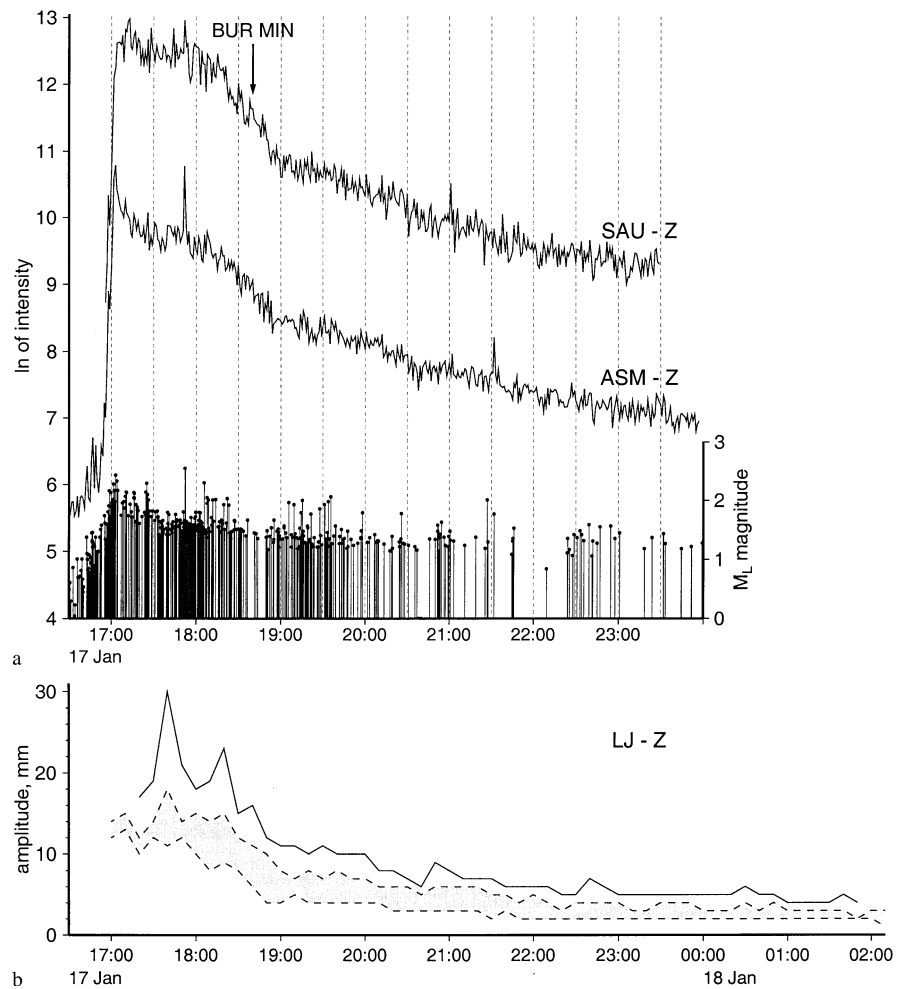
#### Spectral analysis of SAU and ASM data

We used continuous records of the vertical components of the stations SAU and ASM to study the frequency content of the Hekla tremor during the first hours. The tremor has a fluctuating nature, not only in the amplitude but also in its spectrum, as the characteristic spectral peaks typically pop up, remain a minute or a couple of minutes, disappear or get small for some minutes, and reappear as major peaks. We made continuous spectrograms, with the resolution of 0.05 Hz, by making non-overlapping spectra over 1-min-long samples of the records. These are shown

both in three-dimensional view (Figs. 6a and 7a) and in contour plots (Figs. 6b and 7b). We also made a schematic spectrogram for the station SAU by stacking the spectra of five successive minutes (Fig. 8).

Both the stations observed that the tremor was within a well-defined spectral band at 0.5–1.5 Hz. This is in the lower end of the range which has been observed for volcanic tremor in general, mainly 1–9 Hz at active volcanoes around the world (McNutt 1994b). The spectra settled to this band very quickly, only a few minutes after the onset of the eruption. The spectra remained like this all the time during the first 7 h of the eruption. The tremor was sharply peaked—typically there were one dominant peak and a couple of other, outstanding peaks. The amplitudes of the peaks decreased with time but the spectral range remained the same.

**Fig. 5** **a** Tremor intensity observations of SAU and ASM, 17 January 1991. For the graph the seismic data of the vertical components are band-pass filtered between 0.5 and 5.0 Hz. The intensity is calculated as averaged energy over 60-s intervals, and its  $\ln$  logarithm is plotted. The earthquakes related to the onset of the eruption are presented *below*, their magnitude scale is on the *right side*. The eruption started at about 17:00. The moment of the turning point at the strain station BUR is marked with an *arrow*. **b** The amplitudes of the analog station LJ are shown for comparison. In this plot the *shaded area* shows the representative peak-to-peak amplitudes, and the *solid line* the maxima during 10-min-long periods



At the nearer station, SAU, the spectrum remained at its characteristic band from about 17:05 on until the end of the dataset (~23:30). Practically all the maximum peaks were at the band of 0.7–0.9 Hz, however, during the first 2 h in the lower half, and later in the upper half of this band (Figs. 6a, b and 8). Most of the notable peaks existed at the band of ~0.6–1.2 Hz.

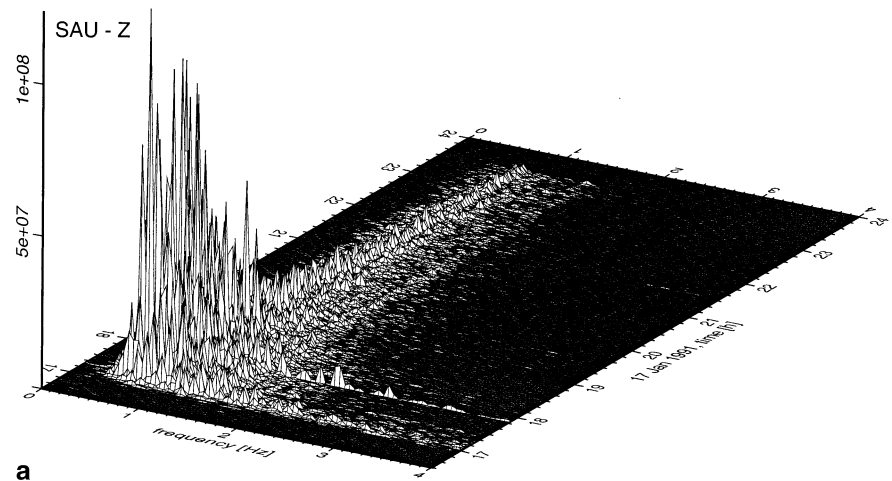
During the first hour, until 18:10, the spectral peaks of SAU had their highest amplitudes. All the maximum peaks were at 0.6–0.8 Hz, and a peak at 0.75 Hz remained highest most of the time. Prominent peaks existed also at 0.7, 0.8, 0.85 and 0.9 Hz. At 18:00 the dominant peak switched to 0.7 Hz where it continuously stayed until 18:35. Then, suddenly the maximum peak switched to 0.9 Hz for some 10 min. This happens also to be the time when strain at the strain station BUR went from contraction to expansion (Linde et al. 1993). Later the location of the maximum peaks switched back to 0.7 Hz and stayed there until 19:00 but after that the location of the highest peak varied in the band of 0.7–0.9 Hz. Around 19:00 all the maximum peaks “disappeared” for a few minutes, as the peaks had considerably smaller amplitudes than during the minutes before and after (Fig. 8).

This was the time of a clear kink in the intensity graph of SAU (Fig. 5a).

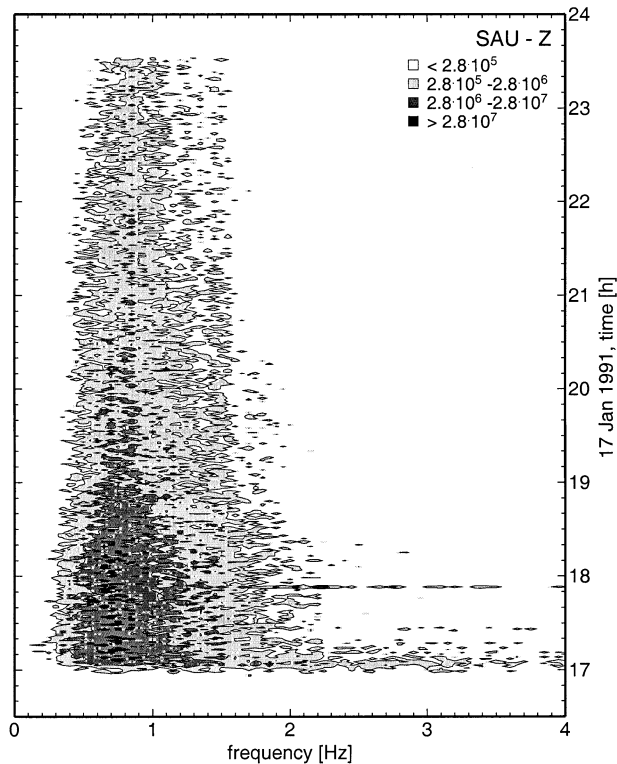
After 19:20 a persistent dominant peak appeared at about 0.85 Hz in the SAU spectrum (Fig. 6a, b). It disappeared for some minutes but then reappeared again at the same frequency. However, until about 20:40, the 0.7 Hz peak occasionally dominated (often when the 0.85-Hz peak was momentarily absent). Thus, the major spectral peaks still were within the same main band, 0.7–0.9 Hz, as earlier but the dominance had switched to 0.8–0.9 Hz. From about 20:40 the persistent major peak of the SAU spectrum was the one at about 0.85 Hz. It fluctuated slightly a few hundredths of hertz and sometimes the maximum skipped to 0.8 or 0.9 Hz. However, the other spectral characteristics, i.e. typical frequency band, and location and existence of typical peaks, continued until the end of the dataset. In the SAU spectrum the high semicontinuous peaks at 0.7 and 0.85 Hz are most apparent. Some other peaks are also prominent at 1.0, 1.25, and 1.45 Hz, although they are never as dominant as the ones at lower frequencies.

The overall structure of the spectrum of the Hekla tremor at the station ASM, 15 km further away, is similar to that of SAU but in the details the spectra differ. The

**Fig. 6a, b** A spectrogram of the vertical component data at the station SAU for the first hours of the eruption: **a** three-dimensional view, and **b** plane view with contour lines (the amplitude scale is arbitrary). The spectrum is a fast Fourier transform power spectrum. The data consist of detrended and demeaned 60-s-long non-overlapping time windows with a 0.5-s cosine taper. No filtering is done. The abscissa is the frequency and it is cut at 4 Hz because peaks above it are of negligible size. The ordinate is the time, from 16:30 on 17 January until midnight



**a**



**b**

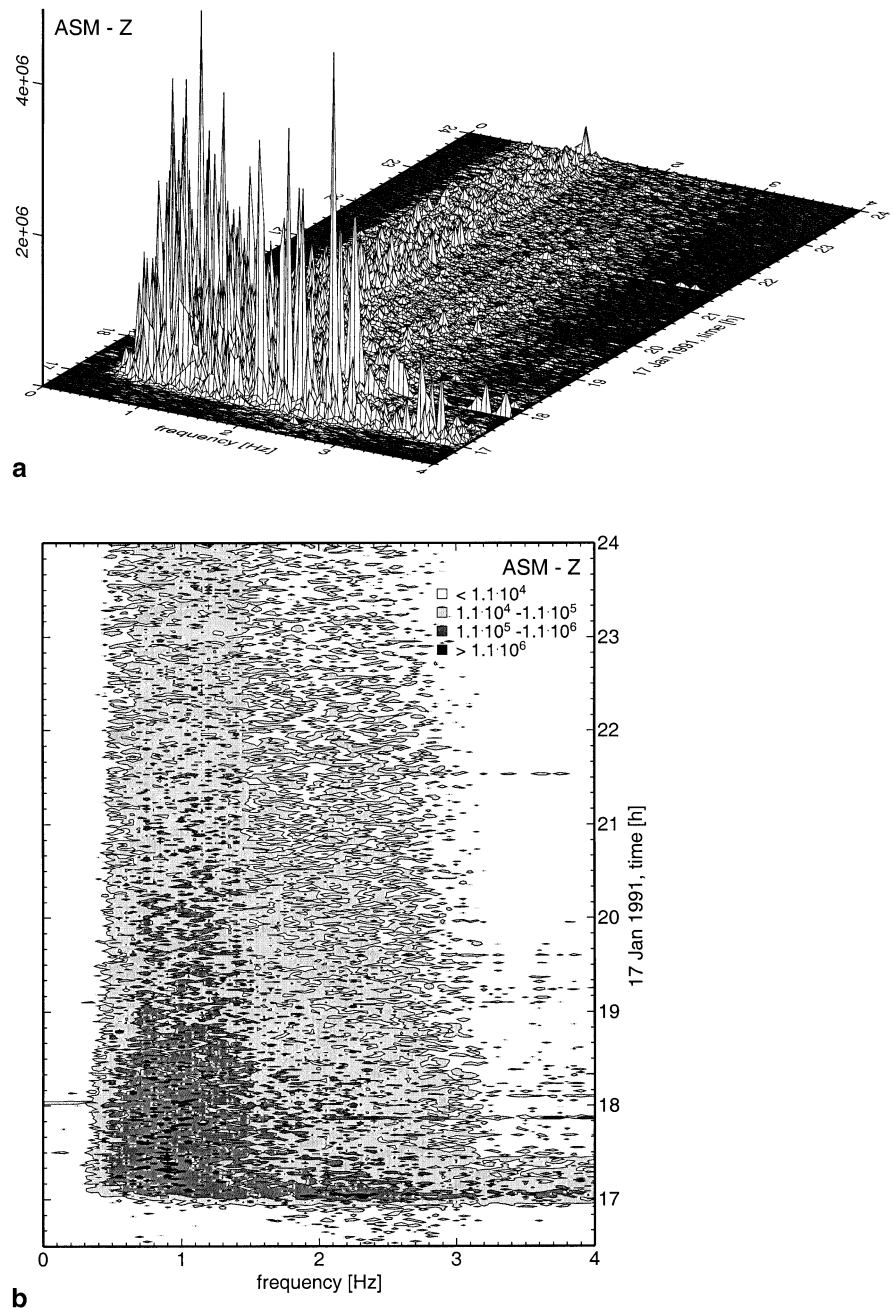
tremor quite effectively attenuates with distance, as the Hekla earthquakes appear more clearly amid the tremor at ASM than at SAU. During the first minutes after 17:00, the numerous earthquakes dominated the ASM spectrum. Later the tremor took over, although the largest earthquakes continued to show their fingerprint in the ASM spectrum. Throughout the dataset, the location of maximum peaks within the band varied somewhat, although the same peaks existed most of the time. The most persistent peaks were 0.75 Hz at 17:40–20:00, 0.85 Hz at 18:45–24:00, and 1.2 Hz at 20:30–23:45. No tremor peak was as persistently dominant as the one at 0.85 Hz at SAU.

In the beginning, at 17:05–18:00 when the tremor was at its maximum, the highest spectral peak at ASM was at about 0.9 Hz. A more persistent peak, but not as high, existed at 0.7 Hz from 17:05. It occasionally popped up until 18:20, after which it was not prominent. At about 17:20 a similarly persistent peak at 0.75 Hz entered but this one survived with varying size until the end of the dataset. Another clear peak at 1.1 Hz existed in the spectrum during the first hour of the eruption.

At the time when the tremor intensity started to diminish, from about 18:00 (Fig. 5a), the band of maxima at ASM widened to 0.75–1.3 Hz. During the quick decrease of the intensity, ca. 18:00–19:00, the maximum



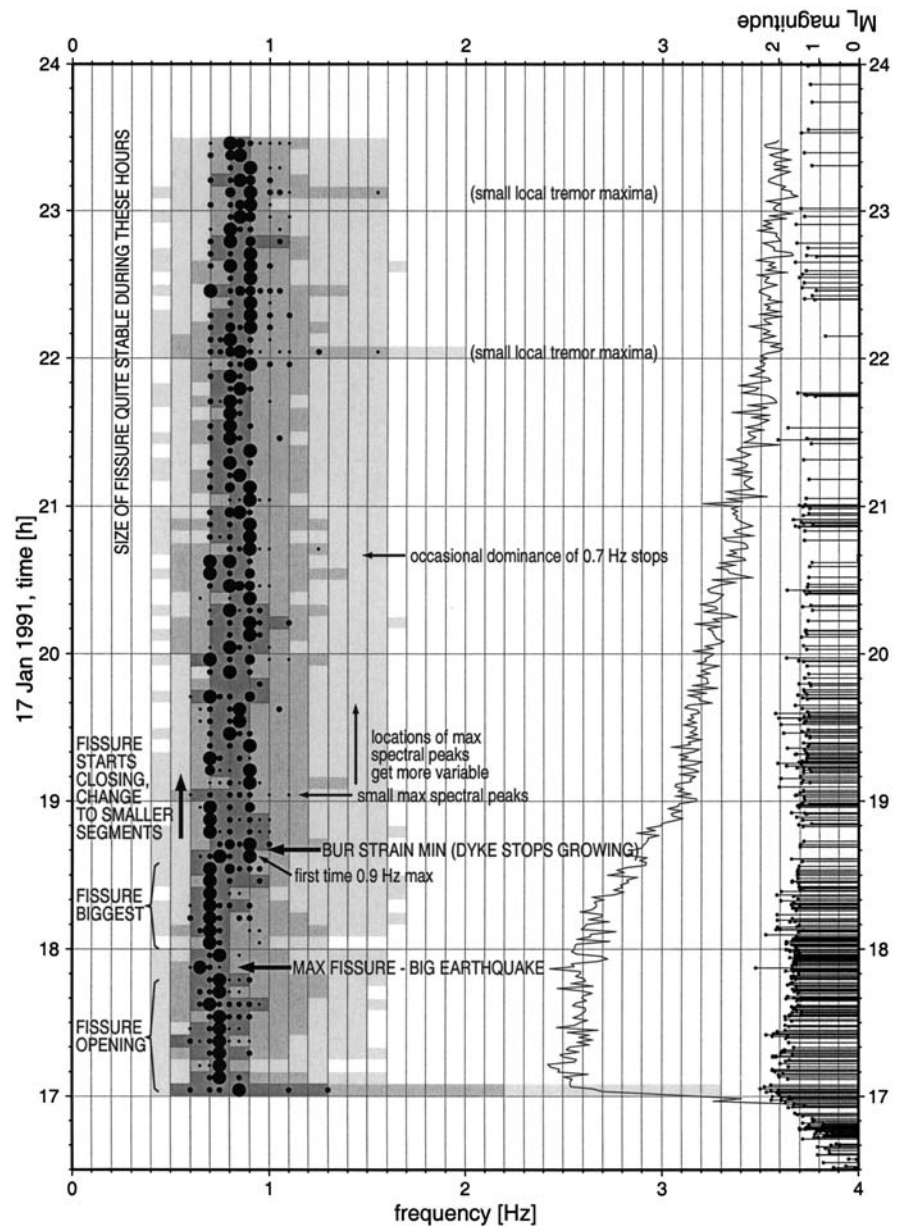
**Fig. 7a, b** A spectrogram of the vertical component data at the station ASM for the first hours of the eruption: **a**) three-dimensional view, and **b**) plane view with contour lines. The data processing is the same as in Fig. 6. Arbitrary amplitude units are the same as for SAU. Note that the amplitude values are far smaller compared to the SAU observations



peaks were located at 0.75, 1.0, 1.1, and 1.3 Hz. At 18:40 the strain station BUR (Linde et al. 1993) had its turning point, coinciding with a clear decline of amplitudes of the spectral peaks of ASM. From 18:40 to 19:10, the main maximum was at 0.75 Hz, and this peak kept on existing as a prominent one until midnight. After about 19:00, the peak at 0.85 Hz appeared in the spectrum of ASM as an occasional maximum. At about 19:00, a kink is visible also in the ASM tremor intensity graph (Fig. 5a). This is not reflected in the spectrum at ASM as dramatically as at SAU. However, at this time the 0.85-Hz peak started to be a major one. After about 19:00 until midnight, distinct peaks were at 0.75, 0.85, 1.0, 1.1, 1.2, and 1.4 Hz.

The spectra of SAU and ASM have both common and different elements—the general appearances are similar but details differ. They both reflect the major turning points of the first hours of the eruption—the turn of the tremor intensity to rapid decrease, the strain change at the local strain station, and change to gentle decrease of the tremor intensity—but differently. Also, the characteristic peaks are similar but appear in different patterns. At SAU they are 0.7, 0.8, 0.85, 0.9, 1.0, 1.25, and 1.45 Hz; at ASM the values are 0.7, 0.75, 0.85, 1.0, 1.1, 1.2, 1.3, and 1.4 Hz. Some peaks coincide exactly, e.g. 0.85 Hz, but the higher ones at 1.2 or 1.25 Hz and at 1.4 or 1.45 Hz do not.

**Fig. 8** Stacked spectra of SAU observations. From 17:00 on, each successive five spectra of 60-s-long records are summed up and prominent peaks presented in a semiquantitative manner. The *largest dot* represents the dominant (on some occasions two dominant) peak(s), the *next largest dots* prominent peaks, the *third largest dots* quite prominent ones, and the *smallest dots* peaks which are not very prominent but still distinct. The peaks of each five-spectra stack are compared to each other, not to peaks at other times. The only exception is the highest peaks at 19:00–19:05 which are marked just with *symbols* as “quite prominent” because they are considerably smaller than peaks immediately before and after. The *shaded bands* show the main area of the spectrum: the *darkly shaded* is the band of outstanding peaks, the *middle shading* the band of prominent peaks (including the former), and the *lightly shaded band* is the area of “visible” spectrum when scaled with the maximum peaks. The intensity graph of SAU and earthquakes of Fig. 5a are shown for comparison. Physical phenomena which can be linked to the observations are suggested in the figure



The different distance from Hekla certainly affects the appearance of the spectra, as is seen from the different attenuation of the tremor and the earthquakes. Different geological conditions below the stations or along the path of seismic signals may magnify the peaks in different ways. The seismic rays to ASM have to travel a longer path via the heavily faulted South Iceland seismic zone than those going to SAU. Thus, the 0.85-Hz peak which is distinct at both stations after the first 2 h of the eruption is very dominant at SAU but exists much more modestly at ASM. On the other hand, the higher frequency peaks (at 1.0–1.45 Hz) are more prominent compared to the lower frequency peaks (at 0.7–0.9 Hz) at the more distant ASM than at the nearer SAU.

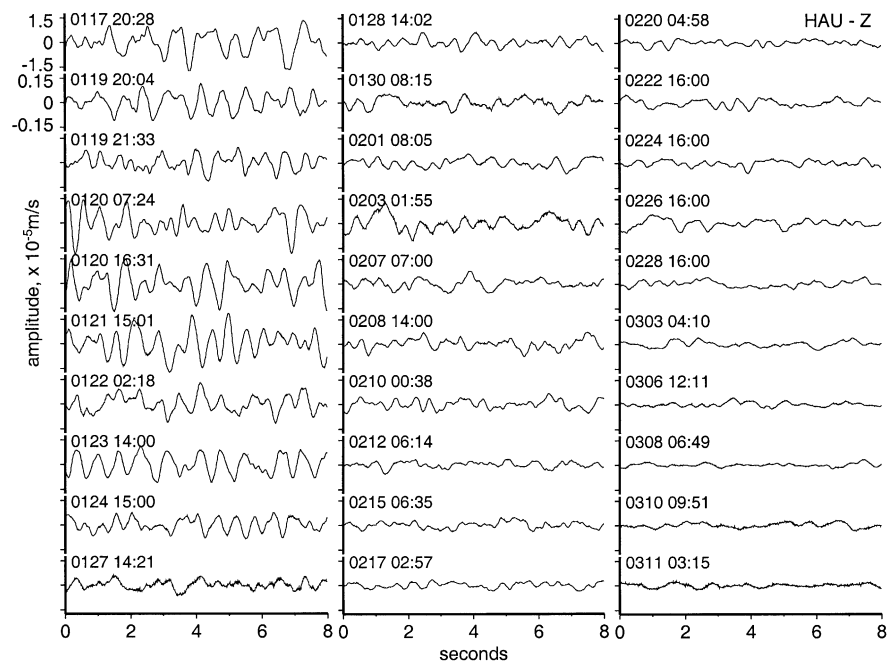
Two analog stations approximately 80 km W–WNW of Hekla also recorded the tremor related to the onset of

the eruption. The tremor is clearly visible until about 18:30 on both, then it quickly decreases until 19:00. From then on it disappears into the noise. The general pattern of the tremor decline is thus similar at all the observing stations.

### The beginning phase of the eruption, first days

This period is best documented by the paper seismograms of the analog station LJ, 35 km ENE from Hekla (Fig. 1). It was the nearest analog station observing the start of the Hekla eruption. The amplitude of the tremor recorded by LJ was measured at 10-min intervals from 17 January on, until it faded out below the background level a few days later. The initial onset of the tremor is difficult to

**Fig. 9** Eight-second-long samples of vertical component seismograms at HAU, with no filtering. The amplitude scale (tick marks at  $\pm 0.15 \times 10^{-5}$  m/s) in all the plots is the same, except that the 17 January sample is plotted at reduced scale (10 times larger than the others). Date and time of the samples are given. Some seismograms (e.g. 27 January) have minor high-frequency noise



determine from these records because the lines are mixed with each other. Reliable measurements can be made from 17:20 on. The tremor amplitude between 17 January at 17:00 and 18 January at 02:00 is presented in Fig. 5b. The first hours before midnight show a similar pattern as the intensity values of the stations SAU and ASM (Fig. 5a).

During the period 02:20–08:10 on 18 January, the magnification of LJ had been turned down and it is not possible to measure the tremor amplitude then. After 08:20, the tremor amplitude remained at the same level as in the first hours of 18 January. However, the slight declining trend of the tremor amplitude continued, but an increase was visible during the period 10:20–18:50 on 19 January. During the next days, the tremor kept on declining gradually and, from 21–22 January on, it was difficult to distinguish between the tremor and the background noise. The records of the station LJ are in harmony with the observation of Guðmundsson et al. (1992) that the eruption was most vigorous during the first 11 h.

### The tremor and its variation during the whole eruption

The digital station HAU is the nearest SIL station to Hekla, and is located 15 km west of the volcano. It recorded only one short sample of data on 17 January but, from 19 January on, there is a tremor dataset of intermittent HAU observations for almost every day of the eruption. The data collected by HAU are the principal material of the study of tremor during the eruption as a whole. In most cases the HAU files which are available were saved because of events, i.e. the files contain

earthquake data and some preceding seconds. Occasionally, 1-min-long files containing solely tremor were also saved. Eight-second-long tremor samples were selected for further studies, in order to maximize the amount of useful data.

Generally there are several observations per day but some days lack data. A representative set of vertical component seismograms of HAU is shown in Fig. 9. The tremor was very vigorous on the seismogram of 17 January, and for convenience it is drawn here at a scale 10 times smaller than the other samples. However, the appearance of the waveform is remarkably similar on that day compared to the following days. During the first days, the tremor was clearly visible as a major element of the seismograms. Its amplitudes fluctuated day by day, and also within one and the same day. The first distinct decline occurred on 22 January. However, the general level of the tremor remained quite high also in the following days.

The volcanic tremor was a major element of the seismograms until about 27 January, after which its amplitude clearly declined. However, around noon on 31 January, there was a distinct increase in the tremor. By the following day this had already subsided. From the beginning of February on, the low-frequency oceanic microseism started to dominate the seismograms, and the highs and lows of the tremor were occasionally detectable. In the beginning of March the tremor was visible on the seismograms only now and then. The tremor disappeared below the detection threshold of HAU, i.e. about  $0.7\text{--}1.4 \times 10^{-7}$  m/s, a few days before the end of the visible eruption.

The intensity of the tremor during the whole eruption was determined, in the same way as for the first evening in Fig. 5a, from all the 8-s-long samples of the tremor

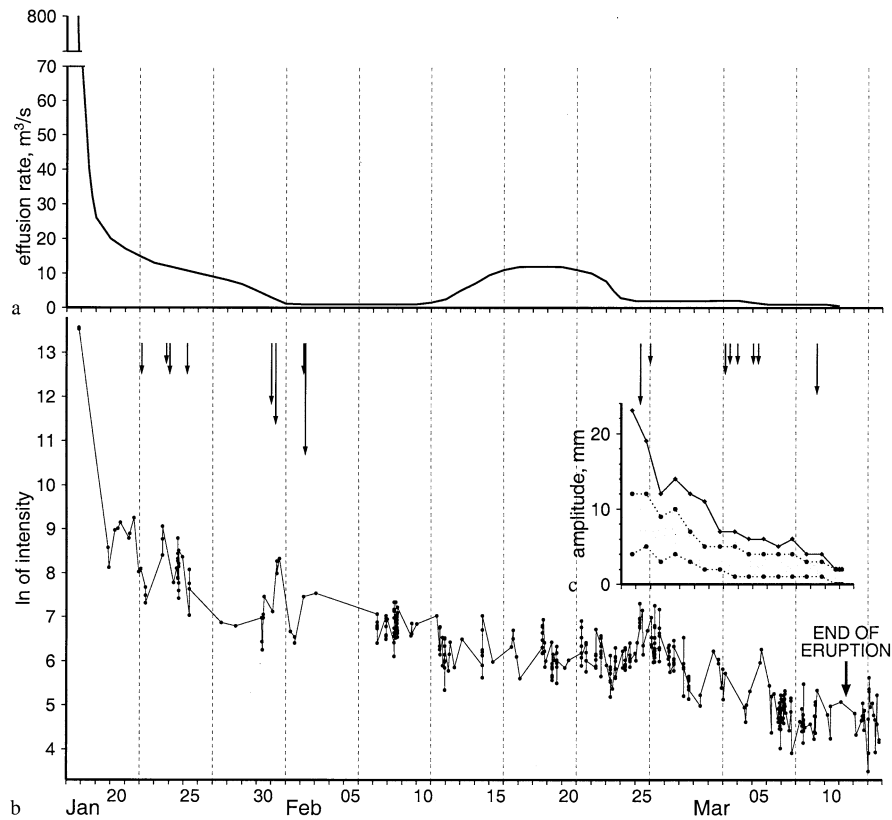


**Fig. 10** **a** Effusion rate throughout the eruption (from Guðmundsson et al. 1992). **b** Semicontinuous tremor intensity observations of HAU throughout the eruption, from the vertical component data. The sample length was 8 s but the method for calculating intensity was the same as used for SAU and ASM in Fig. 5a. The *thick arrow* on 11 March shows the end of the eruption. **c** HE amplitude observations in the last days (starting on 24 February). In the HE plot the *shaded area* shows representative peak-to-peak amplitudes,

and the *solid line* the maxima. There are observation points approximately once a day. *Thin arrows* pointing towards their moment of occurrence show periods of increased tremor level at analog stations LJ (*arrows* in January–early February) and HE (late February–March). The length of the *arrows* tells the length of the periods of increased activity, so that the *shortest arrows* mark 20 min of increased activity, the *longest arrow* 110 min

which were available. The data are band-pass filtered in 0.5–5.0 Hz, and the averaged energy over the 8 s is calculated. This gives a semicontinuous image of the intensity; the corresponding  $\ln$  logarithm values are presented in Fig. 10b. The observations of 17 January (at  $\sim 20:28$ ) give values many orders of magnitude higher than at later times. This is in agreement with the observations of most vigorous tremor and effusion rate during the first hours of the eruption. From 19 January on, the intensity shows rather large variation. There is a general diminishing trend throughout the eruption. On the other hand, comparatively high short-term fluctuations in the tremor amplitude and intensity seem to be characteristic for the whole eruption. The intensity values can fluctuate considerably even within one minute (Fig. 10b). Sometimes there were periods of clearly increased intensities, i.e. on 25–26 February.

Guðmundsson et al. (1992) made observations of the effusion rate during the Hekla eruption and they present the results in a schematic graph, which is here combined with our tremor intensity data in Fig. 10a. They remark that during the eruption its vigour and the tremor

amplitudes correlated. However, the qualitative nature of their graph must be kept in mind when comparing it to the tremor intensity values. The effusion rate graph was constructed by using visual observations, and there are inaccuracies, e.g. due to poor weather conditions or occasional gaps of some days between successive observations.

In general, features of the intensity observations at HAU and the effusion rate graph show similar behaviour. Both have high values in the very beginning of the eruption, and both calm down to much lower level quite rapidly. Later the more slowly declining trend is visible at both until the end of the eruption. However, in details the graphs have some differences. Partly this can be caused by inaccuracy of the effusion rate diagram but differences can also be real. For comparison, Cristofolini et al. (1987), for example, observed volcanic tremor at the Sicilian volcano Etna in June 1980–March 1981 when several eruptions took place. They noted that the highest tremor levels did not always coincide with eruptive phenomena.

Although the volcanic tremor on records of LJ had faded out after a couple of days from the onset of the Hekla eruption, LJ managed to detect some later periods of increased tremor activity. These periods occurred in late January and early February and lasted 20 to 110 min. They are marked with arrows in Fig. 10b. At the end of the eruption, from 24 February on, the analog station HE which is located on Hekla itself is also available. HE has observed similar periods of increased tremor as LJ did in the earlier days. These periods are marked with arrows in Fig. 10b, c as well, and lasted 20 to 60 min. It is somewhat difficult to connect these observations of increased tremor at the analog stations to the intensity values of HAU. They are rather short, and there are only two observation points of HAU (on 2 February and 9 March) which coincide with the analog records (these two show rather high local values). It is possible that the momentary increase of tremor observed by the two analog stations is typical for this eruption. During the times when the tremor was still at moderate level, and LJ could detect a considerable increase, LJ often picked such periods. Also when HE was in use, this seemed to be a frequent phenomenon. During the days in between, there was no suitable station available to detect them.

The very end of the eruption is probably best observed by HE (Fig. 10c). The tremor faded out earlier from the records of HAU 15 km away than from the records of HE on the flank of the volcano. When HE observations start, on 24 February, the volcanic tremor was well visible on its records. During the first days of HE recording, there was a period of general increase in tremor in the observations of HAU. The amplitude values of HE and the intensity values of HAU decline similarly towards 3 March. After that the amplitude remains small and even, however, clearly detectable on HE. The values of HAU still show distinct tremor on 5–7 March, but later on it is hard to say if the tremor can be observed. On HE, although the amplitude values are small, the tremor can still be distinguished until 10 March. The tremor finally disappeared under the detection threshold of HE during the early hours of 11 March. The end of the tremor was followed by a swarm of small earthquakes in the morning. Guðmundsson et al. (1992) put 11 March, at about noon, as the end time of the eruption.

Due to the scarcity of the data we could not make a spectral study of the tremor during the later days of the eruption. Guðmundsson et al. (1992, p. 242) describe results of a small seismic array which was installed near the active crater and operated one day. They detected narrow-band random noise with peak amplitude at about 2.5 Hz, higher than our observations for the first day. They found the tremor consisting of Rayleigh and Love waves with very low velocities.

### Particle motion at the onset of the eruption

The source of volcanic tremor is often inferred to be shallow, and the tremor thus consists mainly of surface

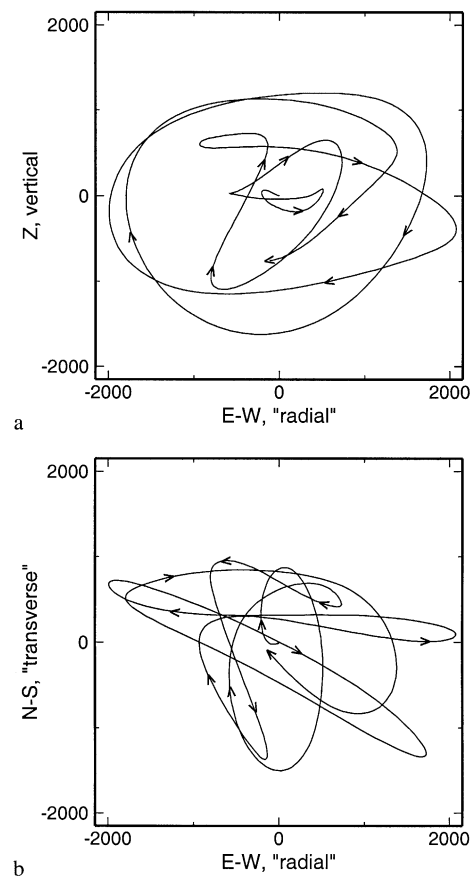


**Fig. 11a, b** Particle motion of a 5.0-s-long sample from station HAU at 20:28:05 on 17 January 1991 (see Fig. 9). The data were band-pass filtered at frequencies 0.5–1.0 Hz, the trend and the mean were removed, and a 0.5-s-long cosine taper was used. **a** The motion in the radial-vertical plane. **b** The motion in the radial-transverse plane. The units are arbitrary, and *arrows* mark the direction of the movement

waves (e.g. McNutt 1986; Gordeev et al. 1990; Gordeev 1992; Goldstein and Chouet 1994; Ripepe et al. 1996). We made particle motion plots for the station HAU. As Hekla, the source of the tremor, is located roughly east of the station, the horizontal north–south and east–west components can be taken approximately as transverse and radial components, respectively. In Fig. 11a, b there is an example of particle motion diagrams of a 5-s-long sample of HAU records at 20:28 on 17 January, in the frequency band 0.5–1.0 Hz. Both of the graphs give somewhat diffuse pictures of the wave content of the Hekla tremor. However, in the radial-vertical plot (Fig. 11a), the retrograde elliptical movement of the Rayleigh waves is obvious. In the radial-transverse plot (Fig. 11b), the particle motion has a clear component of movement in E–W, the direction towards Hekla, this being another indication of possible Rayleigh waves. The particle motion was quite variable in our plots, e.g. a sample at HAU 15 s earlier did not show these motions very clearly. Apparently mixed modes of different wave types are present in the Hekla tremor.

The frequency band plots of all the components of SAU and ASM (Figs. 3a–c and 4a–c) also point to the existence of surface waves. At the frequency bands of 0.5–1.0 and 1.0–2.0 Hz, the attenuation of the vertical component is much bigger than that of the horizontals (compare amplitudes at ASM in Fig. 4a–c). The transverse has highest amplitudes of the three components at both SAU and ASM in the two lower frequency bands, especially in the frequency band of 0.5–1.0 Hz. This is the component where horizontal shear waves and Love waves are best visible, and likely a sign of their existence. This could indicate that Love waves become more important with increasing distance. For comparison, Ereditato and Luongo (1994) have made a study on volcanic tremor at Etna, and they likewise found a large amount of Love waves.

## Conclusions and discussion

A number of possible causes for volcanic tremor have been proposed in the literature. There are models which explain the tremor as the result of resonant effects produced by the geometry of volcanic conduits. Turbulent motion in the vapour–gas–magma mixture makes the volcanic pipes oscillate (e.g. Seidl et al. 1981; Ferrick et al. 1982). In such a case, the frequency content of the tremor may vary with the length of the conduit. Other models suggest that volcanic tremor is produced by vibrations of tensile, fluid-filled, jerkily or suddenly opening cracks (Aki et al. 1977; Chouet 1981). In such models the excess pressure in the fluid generates the trembling. Active participation of the fluid in the form of degassing was added to this modelling by Chouet (1985). In another study, Chouet (1992) states that the tremor is the response of the tremor-generating system to sustained bubble oscillations in the fluid.

Volcanic tremor is often observed to have a peaked spectrum with typically one dominant and a few sub-dominant peaks (e.g. Aki et al. 1977; Chouet 1981; Seidl et al. 1981; Ferrick et al. 1982; Chouet 1985, 1988, 1992). According to Aki et al. (1977), the peaks can be explained as a source effect, such as free oscillations of a magma chamber, or path effects, such as reverberations from the stratigraphic layers. Temporal change of peak frequency during the course of volcanic activity would favour source effect explanations. According to Chouet (1985, 1988), the location of the major spectral peak is dependent on the fluid viscosity and the stiffness of magma-filled cracks. Gordeev et al. (1990) studied volcanic tremor with an array of seismographs at the Klyuchevskoy volcano in Kamchatka. They concluded that the general envelope of the tremor frequency band represents its source, and individual spectral peaks rather reflect individual properties of the medium at the observing stations. Thus, the medium near the stations would act as a stratigraphic filter, and the observed peaks can be quite different at different locations.

Volcanic tremor often begins prior to the actual surface outbreak of an eruption and may extend beyond the duration of surface activity (e.g. Chouet 1981; Montalto et al. 1995). This was not the case at Hekla where the tremor started at the same time as the eruption, and also stopped simultaneously with the eruptive activity. Thus, the tremor observations cannot be used for predicting the Hekla eruptions. The tremor-producing process at Hekla could apparently not start before the connection of the magma conduit with the atmosphere was reached. This supports the explanation of degassing of magma being a cause of the tremor.

During the first hours of the Hekla eruption, the fissure system was changing dramatically and several fissures were active. The effusive activity diminished significantly during the first night and was getting more localized (Guðmundsson et al. 1992; Guðmundsson and Sæmundsson 1992). Although the eruptive activity and tremor intensity were quite variable, the main frequency band of the tremor, both at SAU and ASM, was remarkably stable at about 0.5–1.5 Hz during the first 7 h. However, the individual outstanding peaks within the band were amplified differently at different stations, and the relative amplitude of the peaks changed with time. The idea of Gordeev et al. (1990) of a general spectral envelope of the volcanic tremor and separate peaks being local effects near the stations can be valid to some extent. Still, there are patterns in the locations of the spectral peaks which can be associated with known phenomena in the course of the eruption (see Fig. 8). Thus, we believe that although the station SAU is quite distant from Hekla, we can see features in the tremor records which are source effects. Admittedly, path effects and source effects cannot be distinguished very well with our dataset. For instance, many patterns which are clear in the spectra of SAU get blurred in the spectra of the more distant ASM with a different path.

The dominant peaks at the lower frequency end (<1 Hz) of the characteristic spectral band of the tremor suffer more from attenuation than those in the higher frequency end (>1 Hz). This is surprising, as it is generally assumed that high frequencies attenuate faster than the low ones. Ukawa (1993) has made similar observations as ours at the Ito-oki submarine volcano in Japan. During the 1989 eruption of Ito-oki, volcanic tremor was recorded, with two kinds of predominant spectral peaks, around 1 Hz and between 2 and 7 Hz. Low-frequency waves were dominant at distances less than 50 km, and the higher-frequency waves at more distant stations. Ukawa (1993) states that the former are signals of surface waves trapped and magnified in the sedimentary layers of the sea bottom, and the latter express compressional body waves travelling deeper in bedrock.

If the frequency content of the tremor is dependent on the size of the magma channel, as in the models of Seidl et al. (1981) and Ferrick et al. (1982), a shift of maximum spectral peak should be visible in the beginning phase of the Hekla eruption. Thus, the peak should be at a lower

frequency when there is a larger fissure open, and then change to higher frequency when the magma channel gets smaller.

The general observation that tremor is sharply peaked, having one dominant and several subdominant peaks, is valid for Hekla. The spectral peaks of SAU provide an opportunity to relate the course of the eruption to the tremor (Fig. 8). During the first couple of minutes of the eruption, the numerous earthquakes dominate the spectrum with higher frequencies but, soon, the main peaks jump to the characteristic band of the tremor, 0.7–0.9 Hz. The main peaks remained there the following hours, first in the lower end, 0.7–0.8 Hz, and later in the higher end, 0.8–0.9 Hz. During the first tens of minutes of the eruption when the fissure was opening, the main peak was at 0.75 Hz. After 17:50, the  $M_L$  2.5 earthquake occurred which could be the sign that the fissure had reached its maximum. At this time the major spectral peak jumped to lower frequency, 0.65 Hz. During the first half an hour after 18:00, the main peak was at 0.7 Hz, and this can be interpreted to be the time when the fissure was at its biggest. After that the intensity of the tremor started its rapid decrease. After 18:30 the major peak at 0.9 Hz appeared for the first time. Soon after this, the strain station BUR observed a change which showed that the dyke had stopped growing. The fissure started to close and to be divided into smaller segments. The main spectral peak remained at 0.7 Hz. The spectrum changed drastically around 19:00, at the time of a kink in the intensity diagram. For some minutes all the spectral peaks became considerably smaller than immediately before and after. The peaks soon recovered but after this they had a more diffuse pattern and the main peaks at 0.8–0.9 Hz became common. Occasional dominance of the 0.7-Hz peak more or less stopped around 20:40, and later the dominant peaks were at 0.8–0.9 Hz. This could indicate that the fissure remained quite stable as from 20:40. In Fig. 6a, b the outstanding peak is at 0.85 Hz. However, in the stacked plot in Fig. 8, the main peak fluctuates at 0.8–0.9 Hz. This is caused by the fact that the 0.85-Hz peak seldom was continuous for longer than a couple of minutes.

Tremor observations of Guðmundsson et al. (1992) compared to ours fit, at least qualitatively, to the idea that large eruptive channels produce lower peak frequencies and small channels higher frequencies. Their study was made in a later stage of the eruption when the activity was restricted to one crater, and it showed a higher peak frequency (2.5 Hz) than ours.

Chouet (1981) states that a shift in the dominant tremor frequency does not have to reflect a growing crack but may result from a change in source location, i.e. a change in the path of magma during the course of the eruption. Also, according to Chouet (1985), lowering the fluid viscosity sharpens and amplifies the dominant and subdominant peaks, and also shifts the frequency to a higher value. Further, Chouet (1988) mentions that the crack stiffness affects the tremor spectrum. Larger

stiffness shifts the peaks to lower frequencies and decreases their bandwidth.

Rapid changes were characteristic of this Hekla eruption. The earthquakes preceding the onset of the eruption were observed only about half an hour earlier. After the eruption had reached the surface and the tremor started, its spectrum settled in some minutes to its characteristic band at about 0.5–1.5 Hz. On the other hand, the fluctuating nature of the Hekla tremor, both in the short and long term, appears to be an intrinsic feature. This is seen in the seismograms, intensity graphs and spectra throughout the eruption. As stated in Seidl et al. (1981) for the tremors at Etna, the amplitude frequently shows sudden transients where the average amplitude level increases for a few seconds. “Wave packages” lasting some seconds and which are seen in the seismograms of Fig. 2a, b could be similar to these. Seidl et al. (1981) explain this to be caused by transient hydraulic pressure pulses in the magma flow.

The volcanic tremor is sometimes described to be “harmonic” (e.g. Chouet 1985; McNutt 1986; Chouet 1988; Schlindwein et al. 1995) when evenly spaced spectral peaks represent eigenfrequencies, similar to organ pipes. This does not seem to be valid for Hekla.

The earthquakes of the Hekla area attenuated less with increasing distance than the tremor, as is seen in the observations of SAU and ASM. The difference in attenuation suggests that the earthquakes originated deeper than the tremor. The tremor waves have travelled in loose and faulted surface layers, and the earthquake waves in deeper solid layers with lower attenuation.

Effusion rate and tremor intensity during the eruption correlated in a general way but there were differences in details. Although the effusion rate graph in Fig. 10a has an approximate nature, some of the dissimilarities can be real, e.g. a bulge in the effusion rate curve on 11–23 February which is not reflected in the intensity in Fig. 10b. However, rather than comparing these figures to each other and trying to see correlation between them, one should think of them as representing two, somewhat different sides of the magma dynamics. Ferrick et al. (1982) state that only turbulent movement of the magma flow is reflected by the tremor, and steady (or slowly changing) fluid flow is aseismic. Therefore, it is not possible to quantify the total volume of magma flow using seismic data generated during episodes of volcanic tremor. Studies of Cristofolini et al. (1987) indicate that at Mt. Etna magma rises mainly aseismically through the readily open main conduits, which agrees with the generally poor correlation of earthquakes or tremor with eruptive episodes.

After its short-lived, initial plinian phase, the Hekla eruption was not very violent; further the earthquake seismicity was modest after the very beginning. After the first few days of the eruption, lava was observed streaming in only one or a few channels. On occasions the activity increased, and sometimes a thick steam column and considerable explosive activity were observed. Schick (1988, 1992) states that strong tremor is

not necessarily accompanied by strong lava emission, but strong degassing of volcanoes does coincide with strong tremor. In the light of our observations on this Hekla eruption, it is also likely that the Hekla tremor rather reflects the vigour of the eruption than the amount of produced lava.

**Acknowledgements** H. Soosalu was supported by Finnish Cultural Foundation and the Vilho, Yrjö and Kalle Väisälä Foundation of the Finnish Academy of Science and Letters. The Icelandic Meteorological Office provided the digital SIL data. The National Power Company of Iceland funds the analog seismograph network. Comments of two anonymous reviewers improved the manuscript.

## References

- Aki K, Fehler M, Das S (1977) Source mechanism of volcanic tremor: fluid-driven crack models and their application to the 1963 Kilauea eruption. *J Volcanol Geotherm Res* 2:259–287
- Brandsdóttir B, Einarsson P (1992) Volcanic tremor and low-frequency earthquakes in Iceland. In: Gasparini P, Scarpa R, Aki K (eds) *Volcanic seismology*. Springer, Berlin Heidelberg New York, pp 212–222
- Chouet B (1981) Ground motion in the near field of a fluid-driven crack and its interpretation in the study of shallow volcanic tremor. *J Geophys Res* 86:5985–6016
- Chouet B (1985) Excitation of a buried magmatic pipe: a seismic source model for volcanic tremor. *J Geophys Res* 90:1881–1893
- Chouet B (1988) Resonance of a fluid-driven crack: radiation properties and implications for the source of long-period events and harmonic tremor. *J Geophys Res* 93:4375–4400
- Chouet B (1992) A seismic model for the source of long-period events and harmonic tremor. In: Gasparini P, Scarpa R, Aki K (eds) *Volcanic seismology*. Springer, Berlin Heidelberg New York, pp 133–156
- Cristofolini R, Gresta S, Imposa S, Menza S, Patanè G (1987) An approach to problems on energy sources at Mount Etna based on seismological and volcanological data. *Bull Volcanol* 49:729–736
- Einarsson P (1991) Earthquakes and present-day tectonism in Iceland. *Tectonophysics* 189:261–279
- Einarsson P (2000) The seismograph station on Litla-Hekla and the 2000 eruption (in Icelandic). In: *Abstr Vol Geoscience Society of Iceland Spring Meet 2000*, p 41
- Einarsson P, Björnsson S (1976) Seismic activity associated with the 1970 eruption of volcano Hekla in Iceland. *Jökull* 26:8–19
- Einarsson P, Saemundsson K (1987) Earthquake epicenters 1982–1985 and volcanic systems in Iceland. In: Sigfússon ÞI (ed) *Í hlutarins eðli*, Festschrift for Þorbjörn Sigurgeirsson. Menningarsjóður, Reykjavík (map)
- Ereditato D, Luongo G (1994) Volcanic tremor wave field during quiescent and eruptive activity at Mt. Etna (Sicily). *J Volcanol Geotherm Res* 61:239–251
- Ferrick MG, Qamar A, St Lawrence WF (1982) Source mechanism of volcanic tremor. *J Geophys Res* 87:8675–8683
- Goldstein P, Chouet B (1994) Array measurements and modeling of sources of shallow volcanic tremor at Kilauea Volcano, Hawaii. *J Geophys Res* 99:2637–2652
- Gordeev EI (1992) Modelling of volcanic tremor wave fields. *J Volcanol Geotherm Res* 51:145–160
- Gordeev EI, Saltykov VA, Sinitsyn VI, Chebrov VN (1990) Temporal and spatial characteristics of volcanic tremor wave fields. *J Volcanol Geotherm Res* 40:89–101
- Grönvold K, Larsen G, Einarsson P, Þórarinnsson S, Saemundsson K (1983) The Hekla eruption 1980–1981. *Bull Volcanol* 46:349–363
- Guðmundsson Á, Saemundsson K (1992) The Hekla eruption 1991: course of the eruption and the mechanics of Hekla (in Icelandic). *Náttúrufræðingurinn* 61:145–158
- Guðmundsson Á, Óskarsson N, Grönvold K, Saemundsson K, Sigurðsson O, Stefánsson R, Gíslason SR, Einarsson P, Brandsdóttir B, Larsen G, Jóhannesson H, Þórðarson Þ (1992) The 1991 eruption of Hekla, Iceland. *Bull Volcanol* 54:238–246
- Jóhannesson H, Jakobsson SP, Saemundsson K (1990) Geological map of Iceland, sheet 6, South Iceland, 3rd edn. Icelandic Museum of Natural History and Iceland Geodetic Survey, Reykjavík
- Linde AT, Ágústsson K, Sacks IS, Stefánsson R (1993) Mechanism of the 1991 eruption of Hekla from continuous borehole strain monitoring. *Nature* 365:737–740
- McNutt SR (1986) Observations and analysis of B-type earthquakes, explosions, and volcanic tremor at Pavlof Volcano, Alaska. *Bull Seismol Soc Am* 76:153–175
- McNutt SR (1994a) Volcanic tremor amplitude correlated with the volcanic explosivity index and its potential use in determining ash hazards to aviation. *Acta Vulcanologica* 5:193–196
- McNutt SR (1994b) Volcanic tremor from around the world: 1992 update. *Acta Vulcanologica* 5:197–200
- Montalto A, Longo V, Patanè G (1995) Echo-resonance and hydraulic perturbations in magma cavities: application to the volcanic tremor of Etna (Italy) in relation to its eruptive activity. *Bull Volcanol* 57:219–228
- Þórarinnsson S (1967) The eruption of Hekla 1947–1948. I. The eruptions of Hekla in historical times, a tephrochronological study. *Soc Scientiarum Islandica*, Reykjavík, pp 1–170
- Þórarinnsson S, Sigvaldason GE (1972) The Hekla eruption of 1970. *Bull Volcanol* 36:269–288
- Ripepe M, Poggi P, Braun T, Gordeev E (1996) Infrasonic waves and volcanic tremor at Stromboli. *Geophys Res Lett* 23:181–184
- Schick R (1988) Volcanic tremor-source mechanisms and correlation with eruptive activity. *Natural Hazards* 1:125–144
- Schick R (1992) Volcanic tremor: seismic signals of (almost) unknown origin. In: Gasparini P, Scarpa R, Aki K (eds) *Volcanic seismology*. Springer, Berlin Heidelberg New York, pp 157–167
- Schindwein V, Wassermann J, Scherbaum F (1995) Spectral analysis of harmonic tremor signals at Mt. Semeru volcano, Indonesia. *Geophys Res Lett* 22:1685–1688
- Seidl D, Schick R, Ruscetti M (1981) Volcanic tremors at Etna: a model for hydraulic origin. *Bull Volcanol* 44:43–56
- Soosalu H, Einarsson P (2002) Earthquake activity related to the 1991 eruption of the Hekla volcano, Iceland. *Bull Volcanol* 63:536–544
- Stefánsson R, Böðvarsson R, Slunga R, Einarsson P, Jakobsdóttir S, Bungum H, Gregersen S, Havskov J, Hjelme J, Korhonen H (1993) Earthquake prediction research in the South Iceland Seismic Zone and the SIL project. *Bull Seismol Soc Am* 83:696–716
- Stefánsson R, Ágústsson K, Guðmundsson GB, Þorbjarnardóttir BS, Einarsson P (2000) A successful prediction and warning of an eruption in the Hekla volcano, Iceland. In: *Abstr Vol AGU 2000 Spring Meet*, p 442
- Ukawa M (1993) Excitation mechanism of large-amplitude volcanic tremor associated with the 1989 Ito-oki submarine eruption, central Japan. *J Volcanol Geotherm Res* 55:33–50
- Wessel P, Smith WHF (1998) New, improved version of the Generic Mapping Tools released. *Eos* 79:579